Prostate cell differentiation status determines transient receptor potential melastatin member 8 channel subcellular localization and function.

Gabriel Bidaux, Matthieu Flourakis, Stéphanie Thebault, Alexander Zholos, Benjamin Beck, Dimitra Gkika, Morad Roudbaraki, Jean-Louis Bonnal, Brigitte Mauroy, Yaroslav Shuba, et al.

JCI Online First. Published online on May 17, 2007.

Prostate cell differentiation status determines transient receptor potential melastatin member 8 channel subcellular localization and function

Gabriel Bidaux,[1,2] Matthieu Flourakis,[1,2] Stéphanie Thebault,[1,2] Alexander Zholos,[3] Benjamin Beck,[1,2] Dimitra Gkika,[1,2] Morad Roudbaraki,[1,2] Jean-Louis Bonnal,[1,2] Brigitte Mauroy,[1,2] Yaroslav Shuba,[4] Roman Skryma,[1,2] and Natalia Prevarskaya[1,2]

[1]INSERM U800, Equipe labellisée par la Ligue Nationale Contre le Cancer, Villeneuve d'Ascq, France. [2]Université des Sciences et Technologies de Lille (USTL), Villeneuve d'Ascq, France. [3]Department of Physiology, Medical Biology Center, Queen's University of Belfast, Belfast, United Kingdom. [4]Bogomoletz Institute of Physiology, National Academy of Sciences of Ukraine, Kiev, Ukraine.

In recent years, the transient receptor potential melastatin member 8 (TRPM8) channel has emerged as a promising prognostic marker and putative therapeutic target in prostate cancer (PCa). However, the mechanisms of prostate-specific regulation and functional evolution of TRPM8 during PCa progression remain unclear. Here we show, for the first time to our knowledge, that only secretory mature differentiated human prostate primary epithelial (PrPE) luminal cells expressed functional plasma membrane TRPM8 ($_{PM}$TRPM8) channels. Moreover, PCa epithelial cells obtained from in situ PCa were characterized by a significantly stronger $_{PM}$TRPM8-mediated current than that in normal cells. This $_{PM}$TRPM8 activity was abolished in dedifferentiated PrPE cells that had lost their luminal secretory phenotype. However, we found that in contrast to $_{PM}$TRPM8, endoplasmic reticulum TRPM8 ($_{ER}$TRPM8) retained its function as an ER Ca^{2+} release channel, independent of cell differentiation. We hypothesize that the constitutive activity of $_{ER}$TRPM8 may result from the expression of a truncated TRPM8 splice variant. Our study provides insight into the role of TRPM8 in PCa progression and suggests that TRPM8 is a potentially attractive target for therapeutic intervention: specific inhibition of either $_{ER}$TRPM8 or $_{PM}$TRPM8 may be useful, depending on the stage and androgen sensitivity of the targeted PCa.

Introduction

Aberrant cell differentiation is considered to be a key mechanism in the onset of prostate cancer (PCa) and benign prostatic hyperplasia (BPH) (1). In normal prostatic epithelium, cells coexist in many stages in a continuum of differentiated phenotypes, progressing from stem cells to secretory mature luminal cells via a transient amplifying population (2). Deregulated differentiation and proliferation modify prostate epithelial homeostasis and are thus major causes of tumorigenesis (1, 3). One standard therapy for PCa is androgen ablation, which causes tumor regression by inhibiting both proliferation and apical differentiation. However, under antiandrogen therapy, PCa and metastases progress into an androgen-independent stage, causing cancer relapse with a more aggressive phenotype. Therefore, is it critical to understand the mechanisms involved in PCa progression in order to develop reliable prognostic markers and define new therapeutic treatment strategies.

The role of Ca^{2+} in global cancer-related cell signaling pathways is uncontested. Alterations in Ca^{2+} homeostasis increase proliferation (4, 5) and induce differentiation (6) and apoptosis (7–9). According to a growing number of studies, cationic channels of the transient receptor potential (TRP) family represent key players in calcium homeostasis and cell physiopathology (10). In recent years, the TRP melastatin member 8 (TRPM8) channel has emerged as a promising prognosis marker and putative therapeutic target in PCa (11). Indeed, (a) high levels of TRPM8 mRNA have been found in both BPH and PCa compared with normal prostate (NP) epithelial cells (12, 13); (b) significant differences in expression were found for TRPM8, but not for PCa markers prostate-specific antigen (PSA), hK2, and PSCA, between malignant and nonmalignant tissue samples in identified groups of low- and high-grade PCa, suggesting that TRPM8 is a more specific indicator of PCa (14); (c) TRPM8 loss was observed in prostate tissues from patients treated preoperatively with antiandrogen therapy (15); and (d) TRPM8 expression requires functional androgen receptors (ARs) (16). However, despite all the existing evidence on TRPM8 involvement in PCa, the mechanisms of prostate-specific regulation and functional evolution of TRPM8 during PCa progression remain unclear.

Interestingly, although TRPM8 was originally cloned from the prostate (13), recent studies have firmly established its function as a cold receptor in sensory neurons (17), where it has been functionally characterized as a plasma membrane (PM) cationic channel involved in cold-evoked excitation. However, the features of classical plasma membrane TRPM8 ($_{PM}$TRPM8) have not yet been firmly established in prostate cells. While many hypotheses have been put forward, the prostate-specific function of TRPM8 and the role of Ca^{2+}/Na^{+} inflow that it carries in prostate physiology and carcinogenesis remain unknown. Indeed, 2 recent studies (18, 19) functionally characterized

Nonstandard abbreviations used: -6d, 6 days in culture; AR, androgen receptor; BPH, benign prostatic hyperplasia; $[Ca^{2+}]_c$, cytosolic Ca^{2+} concentration; $[Ca^{2+}]_{ER}$, ER Ca^{2+} content; CK, cytokeratin; $_{ER}$TRPM8, endoplasmic reticulum TRPM8; HEK-TRPM8 cell, HEK293 cell with inducible TRPM8 expression; LNCaP, lymph node carcinoma of the prostate; NP, normal prostate; PCa, prostate cancer; PM, plasma membrane; $_{PM}$TRPM8, plasma membrane TRPM8; PrPCa, prostate primary cancer (cell); PrPE, prostate primary epithelial (cell); PSA, prostate-specific antigen; siTRPM8, siRNA against TRPM8; SOC, store-operated channel; SOCE, store-operated Ca^{2+} entry; TA/I, transit amplifying/intermediate (apical epithelial cells); TRP, transient receptor potential; TRPM8, TRP melastatin member 8.

Conflict of interest: The authors have declared that no conflict of interest exists.

Citation for this article: *J. Clin. Invest.* doi:10.1172/JCI30168.

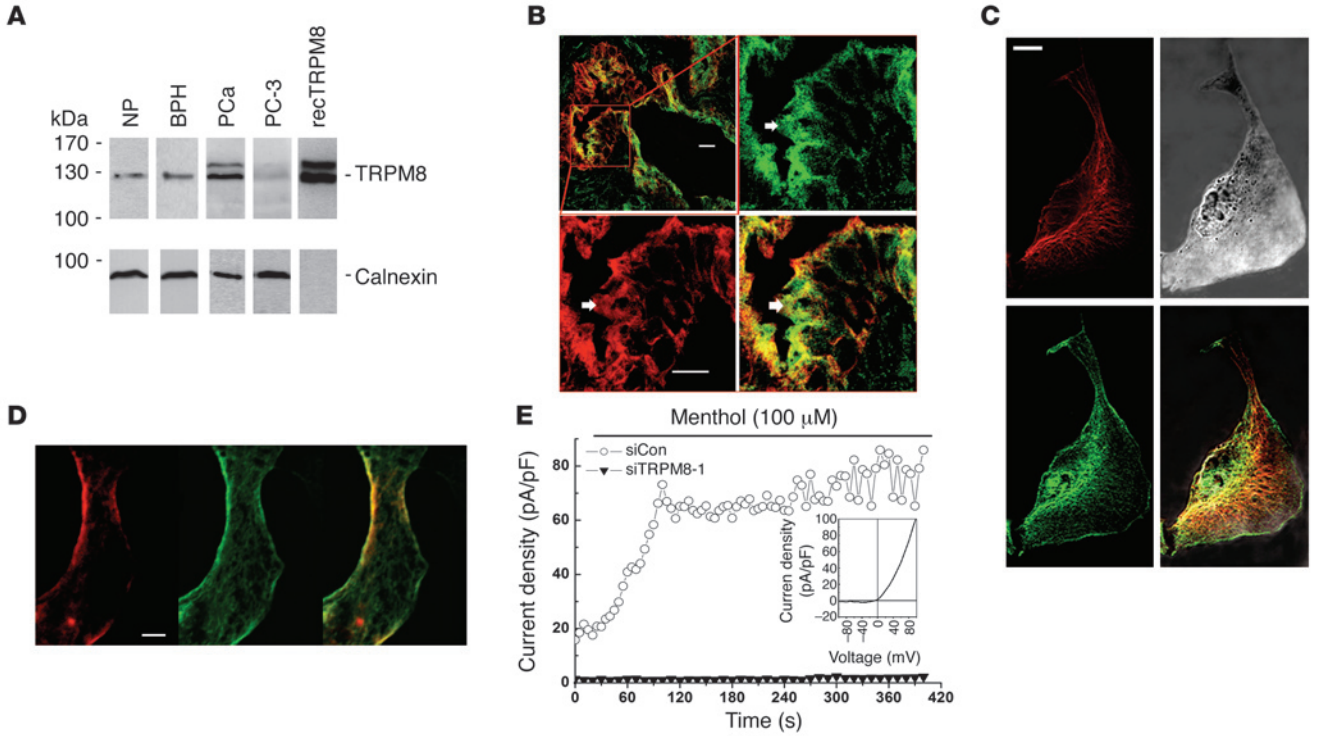

Figure 1
TRPM8 channel expression and activity in human prostate cells. (**A**) Immunoblot showing detection of 128-kDa protein in representative human NP, BPH, and PCa samples. PC-3 cells were used for negative control; detection of recombinant (rec) TRPM8-His fusion protein was used for positive control. Calnexin was used to control the amount of proteins. (**B**) Confocal examination of immunohistochemical sections reporting specific expression of the TRPM8 protein (green) in CK18-positive (red) cells in PCa. Arrows denote TRPM8 expression on the luminal side membrane of apical epithelial cells. Boxed area in top left panel is shown at a higher magnification in the other panels. (**C**) Representative confocal image of a PrPE cell from human BPH showing colocalization of TRPM8 (green) with CK18 (red) 6 days after tissue dissociation. Note that a thin green signal was localized on PM. Top right panel shows the cell viewed with transmitted light. (**D**) PM localization of TRPM8 (green) in PrPE cells was confirmed by its colocalization with membrane marker CD10 (red). (**E**) Representative time courses of menthol-activated i_{TRPM8} in PrPE cells transfected with 50 nM of either siTRPM8 or scramble siRNA (siCon). Inset shows the representative current/voltage relationships of the menthol-activated membrane currents. Scale bars: 10 μm.

the TRPM8 channel in the human PCa lymph node carcinoma of the prostate (LNCaP) cell line. In these cells TRPM8 is highly expressed, but is most exclusively localized in the ER membrane, where it acts as an ER Ca^{2+} release channel that supports the androgen-dependent component of store-operated Ca^{2+} entry (SOCE). However, $_{PM}$TRPM8 is not functional in LNCaP cells. These findings raise a number of intriguing questions. Does prostatic TRPM8 act exclusively on the ER? What mechanisms determine PM versus ER localization? How is TRPM8 function regulated during prostate cell differentiation and carcinogenesis? In light of our previous findings concerning the differential involvement of ER Ca^{2+} release and PM Ca^{2+} entry in the proliferation and apoptosis of PCa cells (5), modifications in TRPM8 localization and activity during carcinogenesis could explain the aberrant cancer cell growth phenotype. Therefore, understanding TRPM8 function in PCa is crucial for making justified conclusions regarding use of this channel as a diagnostic and therapeutic target.

The present study was designed to investigate how TRPM8 localization and activity are regulated depending on the differentiation and oncogenic status of prostate primary epithelial (PrPE) cells. We applied a combination of electrophysiology, Ca^{2+} imaging, and molecular and cell biology approaches to primary cultures of human NP, BPH, and PCa epithelial cells. Our findings show, for the first time to our knowledge, that only highly differentiated PrPE luminal cells expressed functional $_{PM}$TRPM8 channels. Importantly, prostate primary cancer (PrPCa) cells obtained from in situ PCa biopsies were characterized by $_{PM}$TRPM8-mediated current density that was significantly stronger than that of NP or BPH cells. This $_{PM}$TRPM8 activity was abolished in dedifferentiated PrPE cells that had lost their luminal secretory phenotype. In contrast, endoplasmic reticulum TRPM8 ($_{ER}$TRPM8) remained functional regardless of the differentiation status of prostate cells. This differential regulation of TRPM8 activity can be explained by the complex regulation of $_{ER}$TRPM8 and $_{PM}$TRPM8 isoforms by ARs. Considering that ER Ca^{2+} content ($[Ca^{2+}]_{ER}$) is known to regulate cancer cell growth, our finding that $_{ER}$TRPM8 was functional in dedifferentiated PCa cells with downregulated AR provides insight into the role of this channel in PCa progression and may be important for developing therapeutic strategies for metastasized PCa. Finally, we propose a model for the differential regulation of $_{PM}$TRPM8 and $_{ER}$TRPM8 during PCa progression.

Results

Expression of functional TRPM8 in human prostate apical epithelial cells. We initially studied TRPM8 protein expression in several human

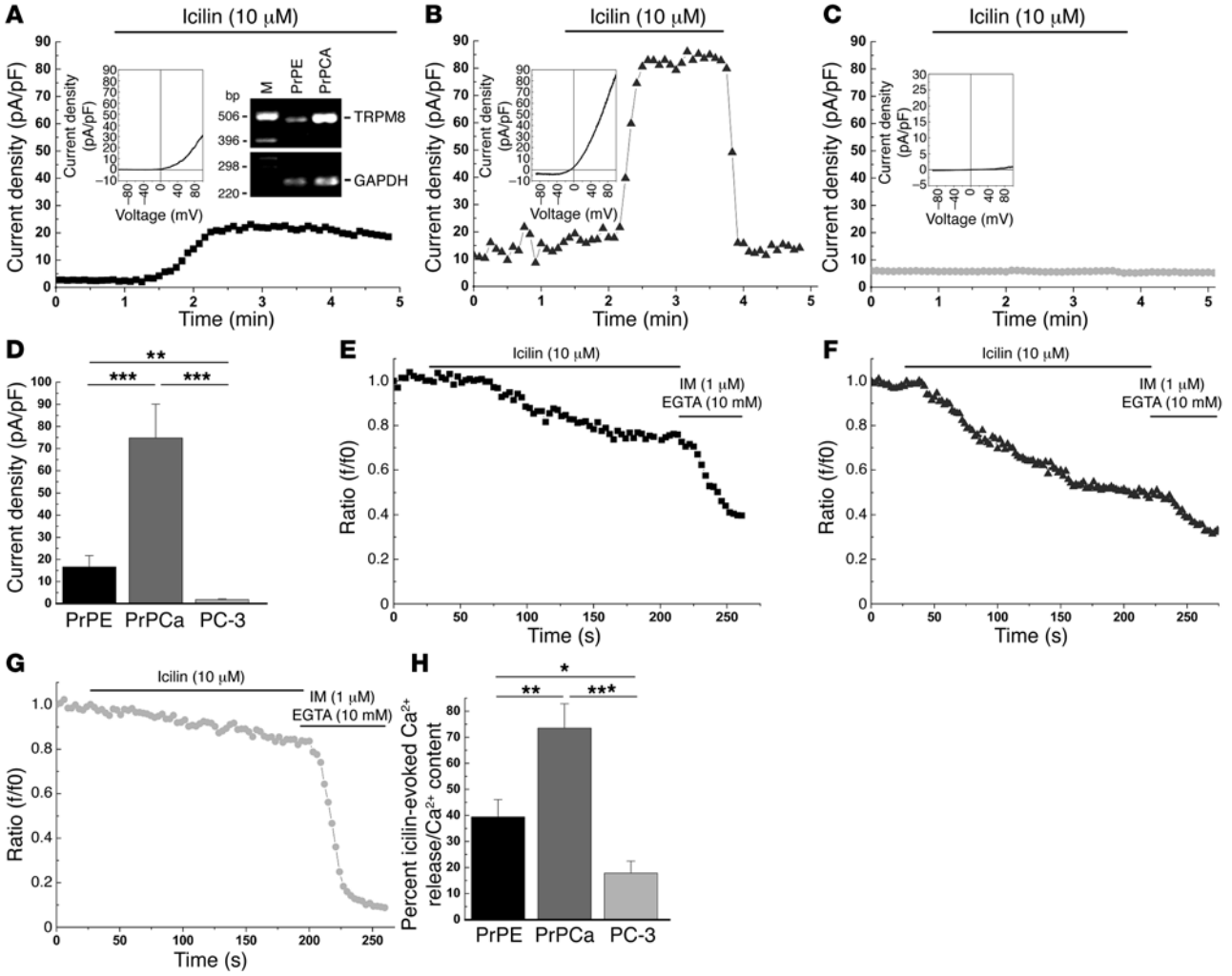

Figure 2

i_{TRPM8} is functional in PrPE cells and presents increased activity in PCa. (**A**–**C**) Representative time courses of icilin-activated i_{TRPM8} in PrPE (**A**), PrPCa (**B**), and PC-3 cells (**C**). Insets show the representative current/voltage relationships of the icilin-activated i_{TRPM8}. Inset in **A** shows an agarose gel indicating the enhancement of TRPM8 expression in PCa. M, protein ladder. (**D**) Cumulative data (mean ± SEM) of maximum currents measured at 100 mV. (**E**–**G**) Typical traces of the estimated passive Ca^{2+} leak induced by 10 μM icilin in digitotin-permeabilized PrPE (**E**), PrPCa (**F**), and PC-3 cells (**G**). IM, ionomycin. (**H**) Cumulative data (mean ± SEM) of icilin-evoked ER Ca^{2+} release. $^{*}P < 0.05$; $^{**}P < 0.01$; $^{***}P < 0.001$.

prostate resection samples by immunoblotting (Figure 1A). As expected, NP, BPH, and PCa extracts expressed 128-kDa TRPM8 protein and its associated glycosylated form (20). Positive control was performed using recombinant TRPM8 protein produced from HEK293 cells with inducible TRPM8 expression (HEK-TRPM8 cells). An androgen-insensitive PCa cell line, PC-3, was also assessed. Although it has previously been reported that TRPM8 is functional in PC-3 cells (19), we did not detect marked TRPM8 protein expression. Immunohistochemical analysis of several NP, BPH, and PCa samples confirmed that TRPM8 colocalized with the apical epithelial phenotype marker cytokeratin 18 (CK18) in acini luminal cells (Figure 1B). PrPE cell cultures were prepared from 3, 6, and 2 NP, BPH, and PCa samples, respectively. As no difference was noted in TRPM8 functional properties between cells from NP and BPH samples, the cells from these 2 sources were unified under the common designation of PrPE cells, while primary epithelial cells from PCa were defined as PrPCa.

TRPM8 protein was expressed in CK18-positive cells, with intense intracellular labeling largely coinciding with expression of this apical phenotype marker (Figure 1C). However, in contrast to our previous findings in LNCaP cells (18), TRPM8 labeling also provided a thin but intense signal on the cell's perimeter, which we attributed to its plasmalemmal localization in PrPE cells. This result was further confirmed by the colocalization of TRPM8 with the CD10 PM marker (Figure 1D).

In view of earlier findings on TRPM8 expression in prostate and prostate-derived epithelial cell lines (18), we investigated whether native prostate epithelial cells exhibit functional responses and analyzed their biophysical properties. Figure 1E shows that PrPE cells responded to the application of menthol (100 μM) at physiological temperatures (36°C) by developing a strong membrane menthol current ($i_{menthol}$). Similar to the i_{TRPM8} in HEK-TRPM8 cells, $i_{menthol}$ was characterized by a current/voltage relationship with sharp outward rectification, close to 0 mV reversal potential (Figure 1E, inset), which

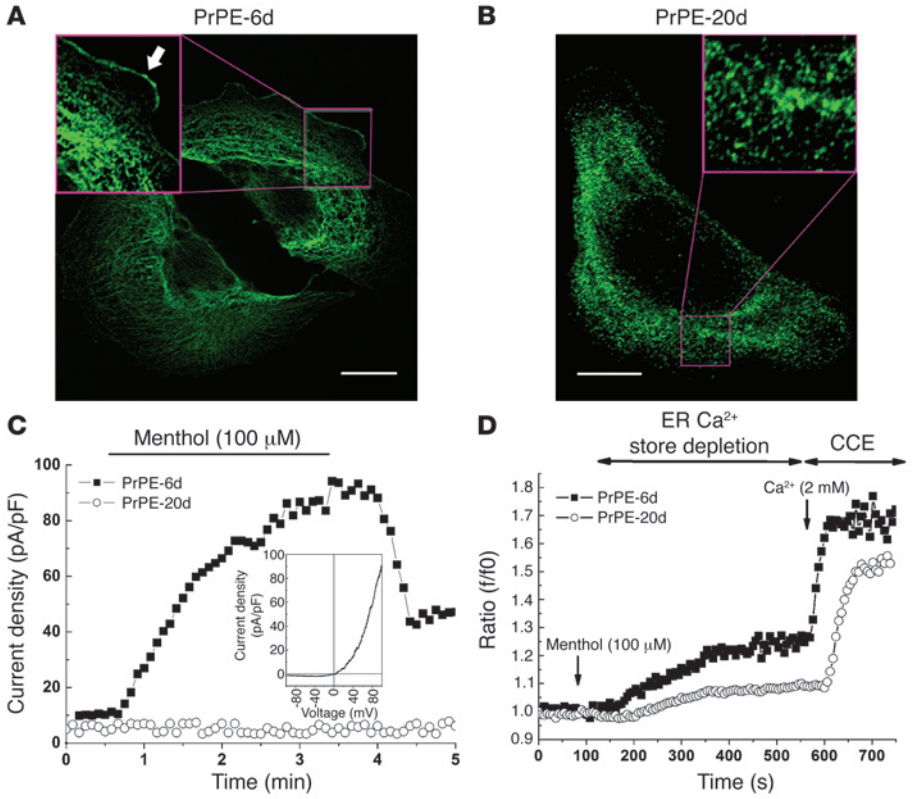

Figure 3
TRPM8 localization and activity in PrPE cells depends on the phenotype of the differentiated epithelial cells. (**A** and **B**) Confocal images showing immunolocalization of TRPM8 in either PrPE-6d (**A**) or PrPE-20d cells (**B**). Higher magnifications of boxed areas are presented in the insets (original magnification, ×600). Scale bars: 10 μm. (**C**) Representative time courses of menthol-activated (100 μM) i_{TRPM8} in PrPE-6d and PrPE-20d cells at 36°C. Currents were recorded from voltage ramps at 100 mV. Inset shows the representative current/voltage relationships of i_{TRPM8}. (**D**) Typical $[Ca^{2+}]_c$ in response to menthol (100 μM) in PrPE-6d and PrPE-20d cells. CCE, capacitative Ca^{2+} entry.

suggests that it was carried through the endogenous $_{PM}$TRPM8 in PrPE cells. In order to demonstrate the association of $i_{menthol}$ with the endogenous TRPM8 in PrPE cells, we used siRNA against TRPM8 (siTRPM8) to selectively knock down TRPM8 mRNA, as was reported in our previous work (18). Figure 1E shows that 48 hours after transfection of PrPE cells with 50 nM siTRPM8-1, $i_{menthol}$ density was almost completely suppressed (siTRPM8-1, 1.83 ± 0.54 pA/pF, n = 11; control, 79.1 ± 5.64 pA/pF, n = 12), indicating a causal link between TRPM8 levels and current magnitude. The siTRPM8 efficiency in TRPM8 knockdown was confirmed by real-time PCR, Western blot, and electrophysiological analysis performed on HEK-TRPM8 cells (Supplemental Figure 2; supplemental material available online with this article; doi:10.1172/JCI30168DS1). Collectively, these data demonstrate that $_{PM}$TRPM8 is functional in PrPE cells and that $i_{menthol}$ can be attributed to TRPM8 activity and thus be defined as i_{TRPM8}.

Transition to PCa increases both $_{ER}$TRPM8 and $_{PM}$TRPM8 activity. Because TRPM8 expression is enhanced in PCa (13–15), but TRPM8 activity in LNCaP cells (derived from metastatic human prostate adenocarcinoma) is found only in the ER membrane (18, 19), we investigated whether PCa development was associated with the shift in TRPM8 localization and function from the PM to the ER by comparing i_{TRPM8} in PrPE and PrPCa cells. Figure 2, A and B, shows membrane currents in representative PrPE and PrPCa cells (the latter derived from a nonmetastatic high-grade PCa, Gleason score 7) before and after exposure to icilin (10 μM) at 36°C. As quantified in Figure 2D, exposure to icilin evoked a 4-fold higher current density in PrPCa cells than in PrPE cells at 100 mV (PrPCa, 74.81 ± 15.31 pA/pF, n = 8; PrPE, 16.62 ± 5.11 pA/pF, n = 6). Enhanced i_{TRPM8} density correlated with higher TRPM8 mRNA levels in PrPCa cells compared with PrPE cells (Figure 2A, inset). We found no current development in response to icilin in the androgen-insensitive PC-3 cell line (Figure 2, C and D).

Next, we sought to determine whether these cell types also reveal TRPM8 activity characteristic of its ER membrane localization. We used compartmentalized fluorescent Ca^{2+} Mag–Fluo-4 dye on permeabilized cells to monitor the effect of TRPM8 activation on $[Ca^{2+}]_{ER}$. In this series of experiments, we used icilin to activate TRPM8, whereas ionomycin and EGTA were used to induce full ER Ca^{2+} store depletion. As shown in Figure 2, E, F, and H, exposure to icilin evoked ER Ca^{2+} release in PrPCa that was 2-fold that of PrPE cells (PrPCa, 73.5% ± 9.37% of total $[Ca^{2+}]_{ER}$, n = 23; PrPE, 39.4% ± 6.68% of total $[Ca^{2+}]_{ER}$, n = 62). Interestingly, icilin in PC-3 cells also induced a measurable decrease in $[Ca^{2+}]_{ER}$ (17.8% ± 4.66% of total $[Ca^{2+}]_{ER}$, n = 29; Figure 2, G and H), which suggests preferred TRPM8 expression and function on the ER membrane, as previously reported (19). These results demonstrated that transition to the PCa did not eliminate $_{PM}$TRPM8 function, as we suggested in our previous report based on LNCaP cell line studies (18), but instead upregulated TRPM8 mRNA expression and enhanced TRPM8 activity in both PM and ER.

TRPM8-mediated PM current disappears during dedifferentiation of prostate apical epithelial cells to the transit amplifying/intermediate phenotype. Because PCa is composed of both transit amplifying/intermediate (TA/I) and apical mature epithelial cells (2, 21, 22), we have investigated TRPM8 regulation during the transition of human prostate epithelial cells from the apical to the intermediate phenotype.

Primary cultures of prostate cells are characterized by the gradual reversion of cell differentiation from the apical phenotype to the TA/I phenotype, which is accompanied by the loss of both AR expression and activity (22). We have previously shown that at least 80% of PrPE cells after 6 days in culture (PrPE-6d) express TRPM8 and apical phenotype markers CK8 and CK18 (16). After 20 days in culture (PrPE-20d), a marked increase in the expression of basal phenotype markers CK5 and CK14 is usually observed, suggesting a reversion of the apical terminally differentiated phenotype to the TA/I phenotype (23, 24). High-magnification confocal images clearly showed the loss of $_{PM}$TRPM8 expression in PrPE-20d cells, as well as deep modifications of intracellular TRPM8 distribution — from a fibrillary pattern to a dotted one — compared with PrPE-6d cells (Figure 3, A and B).

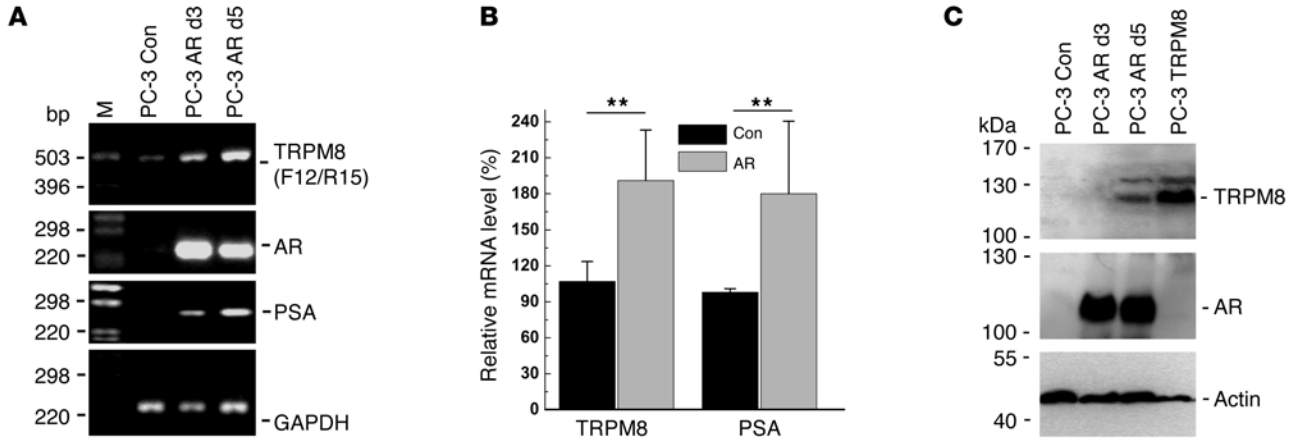

Figure 4

TRPM8 expression is stimulated by AR in PCa cells. (**A**) Agarose gel showing amplification of the 2 TRPM8 amplicons (TRPM8F12/R15), AR and PSA in PC-3 transfected with either empty vector (Con) or AR for 3 or 5 days (d3 and d5, respectively). GAPDH was used as an internal reporter. (**B**) Quantification of PCR experiment in **A**. (**C**) Immunoblotting showing detection of TRPM8 proteins and AR in PC-3 cells transfected with empty vector, with AR for 3 or 5 days, or with TRPM8 encoding vector. Actin was used to control protein loading. $^{**}P < 0.01$.

Thus, reversion of the differentiation characteristic of PrPE-20d cells correlated with the loss of $_{PM}$TRPM8 expression.

Given the change in preferred TRPM8 localization depending on the differentiation status of human prostate cells, we next examined possible differences in the biophysical properties of PrPE-6d and PrPE-20d cell responses to menthol. Figure 3C shows that exposure to 100 μM menthol elicited the development of a strong outward i_{TRPM8} (91.09 ± 9.72 pA/pF at 100 mV, n = 14) only in PrPE-6d cells. Similar results were obtained with icilin (Supplemental Figure 1A), suggesting that $_{PM}$TRPM8 is functional only in mature, fully differentiated human prostate apical epithelial cells.

Imaging experiments on Fluo-2AM–loaded cells aimed at testing for ER membrane TRPM8 activity showed that in the absence of extracellular Ca^{2+}, exposure of both PrPE-6d and PrPE-20d cells to menthol caused a transient increase in the cytosolic Ca^{2+} concentration ($[Ca^{2+}]_c$), obviously the result of ER Ca^{2+} store depletion (Figure 3D). However, the $[Ca^{2+}]_c$ increase appeared much more pronounced in PrPE-6d than in PrPE-20d cells (PrPE-6d, 22.3% ± 5.36%, n = 28; PrPE-20d, 10.4% ± 3.72%, n = 32). This transient $[Ca^{2+}]_c$ increase was followed by sustained $[Ca^{2+}]_c$ elevation upon reintroduction of extracellular Ca^{2+}, a result of store-operated channel (SOC) activity and associated capacitative Ca^{2+} entry, which was also higher in PrPE-6d cells (Figure 3D and Supplemental Figure 1B). These results indicate that TRPM8 is also present in the ER membrane of PrPE cells, where it functions as a Ca^{2+} release channel involved in SOC activation. However, the fact that $_{ER}$TRPM8, unlike $_{PM}$TRPM8, remained functional in cells that lost their apical phenotype suggests that these represent different forms of TRPM8: $_{PM}$TRPM8 is specific to the fully differentiated, apical epithelial cell phenotype, and $_{ER}$TRPM8 does not show preferred expression depending on the differentiation status of prostate epithelial cells. To verify this hypothesis, we used a well-characterized model of apical epithelial cell differentiation consisting of artificial overexpression of AR in the inherently androgen-independent PC-3 PCa cell line.

ARs differentially regulate $_{ER}$TRPM8 and $_{PM}$TRPM8 activities. Given that (a) $_{ER}$TRPM8 activity may take 2 forms depending on AR activity of epithelial prostate cells, (b) classic TRPM8 expression is dependent on the AR (15, 16, 19), and (c) AR controls both the differentiation and proliferation of prostate epithelial cells (25, 26), we next sought to determine the relationship among AR activity, $_{PM}$TRPM8 activity, and $_{ER}$TRPM8 activity.

We investigated whether heterologous AR overexpression in PC-3 cells affects TRPM8 expression and function. First, we compared TRPM8 and AR mRNA expression in wild-type control and AR-transfected PC-3 cells by PCR (Figure 4A). The expression of AR-dependent PSA mRNA served as a control for AR activity. As shown in Figure 4, A and B, control PC-3 cells were found to express very low levels of AR and TRPM8 mRNAs. However, 5 days after AR transfection, quantification of PCR products revealed strong upregulation of TRPM8 (from 107% ± 17% to 191% ± 42%) as well as PSA (from 98% ± 3% to 180% ± 61%) mRNAs (Figure 4B). Western blot experiments showed no specific AR protein expression in the control PC-3 cells and its strong elevation in AR-transfected PC-3 cells (Figure 4C). Classic 128-kDa TRPM8 protein and its posttranslationally modified (glycosylated) 145-kDa form became clearly detectable on the fifth day after AR transfection (Figure 4C). Detection of TRPM8 proteins by Western blot was confirmed on PC-3 cells directly transfected with recombinant human TRPM8 (Figure 4C).

Ca^{2+} imaging and electrophysiological experiments showed that enhancement of endogenous TRPM8 expression in PC-3 cells following AR transfection was paralleled by increased functional responses. Menthol induced a modest decrease in $[Ca^{2+}]_{ER}$ 3 days after AR transfection (18% ± 7.2%, n = 31), which suggests the presence of very low basal TRPM8 activity in the ER membrane in control PC-3 cells, whereas ER Ca^{2+} store depletion by menthol was approximately 1.5-fold that of control 3 days after transfection (i.e., 33% ± 6.77% increase, n = 33), and approximately 3-fold that of control 5 days after transfection (i.e., 53% ± 6.2% increase, n = 28) (Figure 5, A and B). Interestingly, in TRPM8-overexpressing PC-3 cells, menthol induced almost the same ER Ca^{2+} store depletion (61% ± 5.2%, n = 45) as in the PC-3 cells 5 days after AR transfection (Figure 5, A and B).

Figure 5, C–E, demonstrates that PC-3 cells 5 days after AR transfection also acquired the ability to generate classic outwardly rectifying menthol-activated i_{TRPM8} (3.34 ± 0.55 pA/pF, n = 12), which suggests that $_{PM}$TRPM8 expression and function is strictly regulated by the AR. In comparison, the response to menthol in TRPM8-

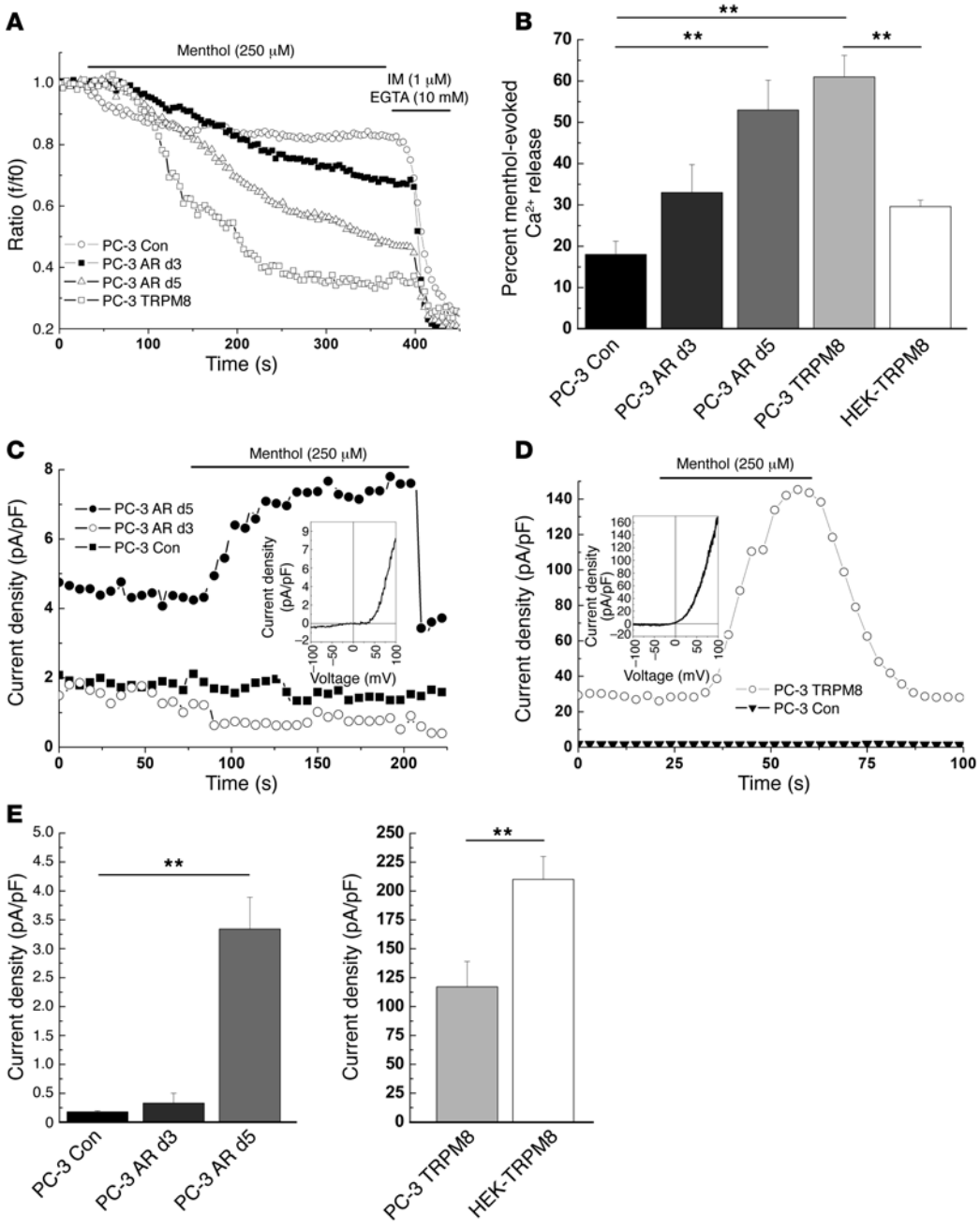

Figure 5
TRPM8 activity correlated with AR expression levels in PC3 cells. (**A**) Typical traces of the estimated ER Ca^{2+} release induced by 250 μM menthol in digitotin-permeabilized control PC-3 cells, PC3 cells transfected with AR for 3 or 5 days, and TRPM8-transfected PC3 cells. (**B**) Cumulative data (mean ± SEM) for percent release from internal Ca^{2+} stores measured at 375 s. (**C** and **D**) Representative time courses of menthol-activated (250 μM) i_{TRPM8} in control PC3 cells and in PC3 cells transfected with AR for 3 or 5 days (**C**) as well as in TRPM8-transfected PC3 cells (**D**). Insets show the representative current/voltage relationships of the baseline and menthol-activated membrane currents. (**E**) Cumulative data (mean ± SEM) of maximum currents measured at 100 mV. $^{**}P < 0.01$.

overexpressing PC-3 cells' outwardly rectifying i_{TRPM8} reached a density as high as 117 ± 22 pA/pF (n = 14; Figure 5, D and E). These data suggest that TRPM8 in PC-3 cells is expressed at some low, baseline level in an AR-independent manner and is exclusively functional in the ER membrane. Furthermore, upon reaching full functionality, the AR promotes the expression of classic AR-dependent TRPM8, which targets both PM and ER membranes. Thus, functional AR seems to be imperative for $_{PM}$TRPM8 activity, while the activity of $_{ER}$TRPM8 may take place even in AR-deficient cells.

To resolve the specific AR dependence of the $_{ER}$TRPM8 and $_{PM}$TRPM8 we observed that (a) although classic TRPM8 mRNA was undetectable in wild-type PC-3 and PrPE-20d cells, menthol and icilin evoked Ca^{2+} release in those cells, (b) TRPM8-overexpressing PC-3 cells presented significantly higher menthol- and icilin-evoked Ca^{2+} release than did HEK-TRPM8 cells (Figure 5, B and E), and (c) TRPM8-overexpressing LNCaP cells did not develop i_{TRPM8} because of ER retention of TRPM8 (18), we hypothesized the existence of 2 TRPM8 isoforms whose function and subcellular targeting are differentially regulated by the AR.

A new TRPM8 isoform may be partially responsible for $_{ER}$TRPM8 activity. It is important to note that in the pioneering paper by Tsavaler et al. (13), the expression of 2 different transcripts (6.2 kb and 5.2 kb) of TRPM8 was demonstrated in the prostate, although only the longer one has been cloned to date. Thus, we hypothesized that the expression of a truncated TRPM8 splice variant could be responsible for basal, AR-independent $_{ER}$TRPM8 activity. Figure 6A shows the alignment of known TRPM8 mRNAs and the putative genomic structure of the *trpm8* gene. Although *trpm8* is composed of 27 exons, only 24

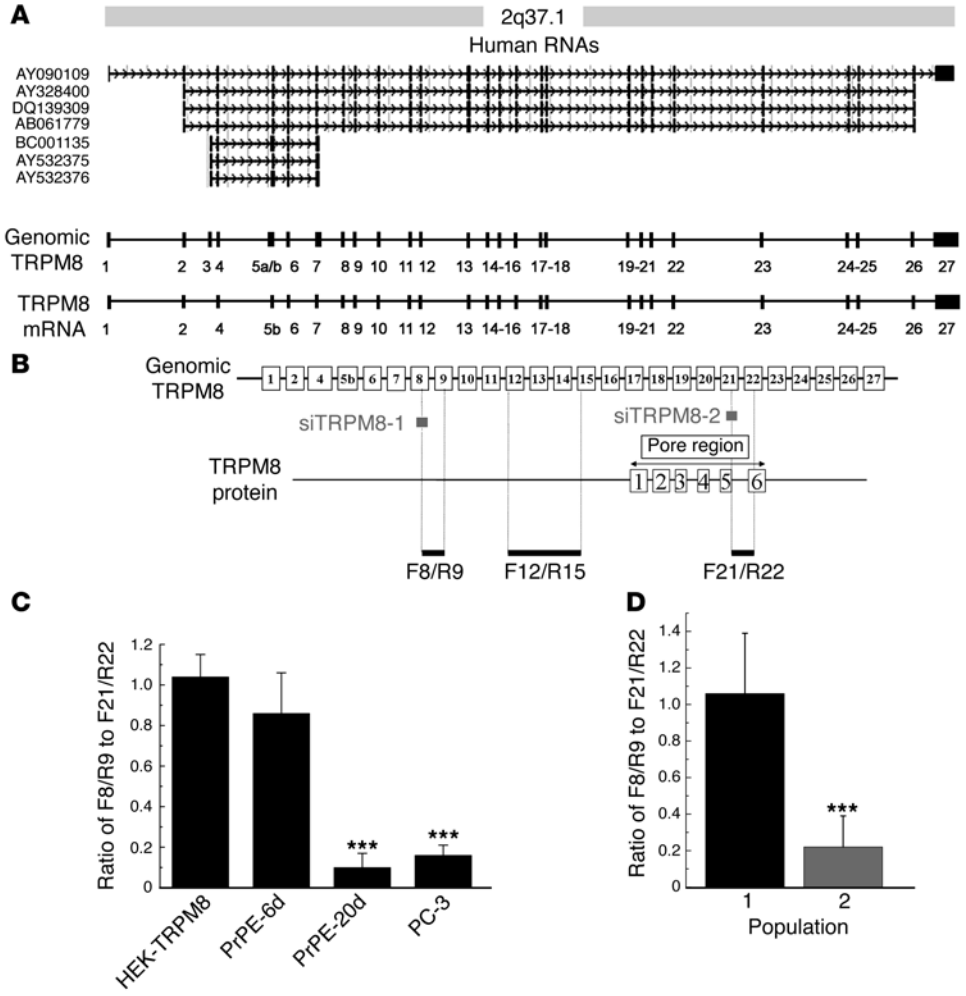

Figure 6
The *trpm8* gene encodes for classical TRPM8 channel and a putative truncated TRPM8 splice variant. (**A**) The *trpm8* gene localized on chromosome 2 in position 37.1. Alignments of several TRPM8 mRNAs and proposed structures of TRPM8 genomic DNA and mRNA to scale. (**B**) Genomic map of TRPM8 (not to scale; numbered boxes denote exons) with its associated protein structure (boxes 1–6 represent putative transmembrane domains). The 3 pairs of PCR primers and siTRPM8-1 and -2 are aligned with their matching exons. (**C**) Real-time analysis of exons 8 to 9 amplicon (F8/R9) and exons 21 to 22 amplicon (F21/R22). Data are presented as a ratio of F8/R9 to F21/R22. HEK-TRPM8 cells represent the control condition with only 1 TRPM8 mRNA variant. (**D**) Ratio of TRPM8 F8/R9 to F21/R22 expression normalized to hypoxanthine-guanine phosphoribosyl transferase (HPRT) expression after quantification of PCR products obtained from single cells. Each population is represented by 10 prostate apical epithelial cells. ***$P < 0.001$.

of them are involved in the formation of cold/menthol receptor (13). Using differential real-time PCR, we measured the expression intensity of the amplification products using the primer pairs F8/R9 (flanking the region between exons 8 and 9) and F21/R22 (flanking exons 21 and 22) in PrPE-6d and PrPE-20d cells (Figure 6B). Standardization of amplifications had previously been validated on TRPM8 DNA and cDNA from HEK-TRPM8 cells (18). The proportion of each amplicon was used to determine the ratio of F8/R9 (representing the classical TRPM8) to F21/R22 (representing the classical TRPM8 and TRPM8 isoform) (Figure 6C). We found that differentiated PrPE-6d cells were characterized by a F8/R9-to-F21/R22 ratio close to 1 (i.e., 0.86 ± 0.2), which was comparable to that of HEK-TRPM8 cells (1.04 ± 0.11), while dedifferentiated PrPE-20d cells and PC-3 cells showed ratios of 0.10 ± 0.07 and 0.16 ± 0.05, respectively (Figure 6C). These results indicated that the level of classic TRPM8 mRNA in PC-3 and PrPE cells constitutes no more than 16% of the total TRPM8 mRNA. Thus, we hypothesized that the expression of the truncated splice variant may explain our functional result.

In order to determine to what degree these 2 mRNAs were present in individual cells, we performed single-cell real-time PCR on apical prostate epithelial cells. These experiments enabled us to identify 2 populations of cells, for which the calculated ratios of F8/R9 to F21/R22 were 1.06 ± 0.33 and 0.22 ± 0.17 (Figure 6D). In the framework of our hypothesis, we posited that the former population was likely to express predominately the classic TRPM8, while the latter would probably express both classic TRPM8 and truncated TRPM8 mRNAs (Figure 6D).

We also developed specific siRNA directed against exon 8 (i.e., siTRPM8-1) or exon 21 (i.e., siTRPM8-2) in order to selectively ablate either the classic TRPM8 mRNA or both the classic and the truncated TRPM8 mRNAs. We performed experiments on PC-3 cells and quantified TRPM8 mRNA levels by real-time PCR. Both siTRPM8-1 and siTRPM8-2 specifically suppressed the classic TRPM8 mRNA (7-fold and 3-fold decrease, respectively), as assayed by RT-PCR with the F8/R9 pair of primers (Figure 7A). We performed $[Ca^{2+}]_{ER}$ measurements to study the effect of siRNAs on $_{ER}$TRPM8 activity. Figure 7B shows that only PC-3 cells transfected with siTRPM8-2 were characterized by decreased menthol-evoked Ca^{2+} release, which constituted 30.19% ± 16.42% that of control cells. The same experiments conducted on PrPE-20d cells transfected with siTRPM8-2 provided a similar reduction (22.58% ± 21.48% of control; Figure 7C). Control experiments conducted in HEK-TRPM8 cells under the same conditions revealed similar potency in the 2 siRNAs. However, siTRPM8-1 induced weak silencing (2-fold decrease) compared with the strong (10-fold) siTRPM8-2–mediated decrease of TRPM8 mRNA detected with the F21/R22 primer pair, although both of them had the same efficiency (10-fold decrease) in HEK-TRPM8 cells (Figure 7D and Supplemental Figure 2A). Control experiments on

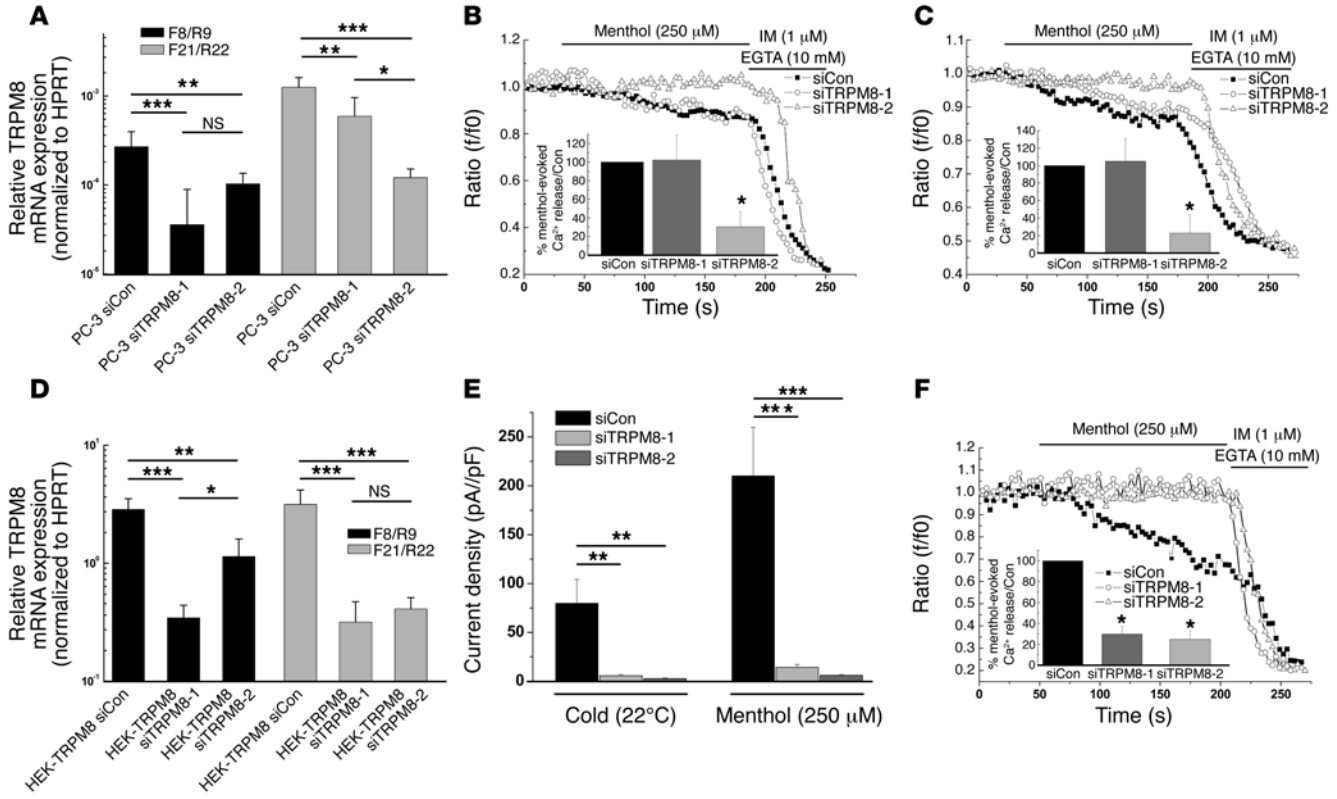

Figure 7

Specific siRNA-mediated ablation of either classical TRPM8 or total TRPM8 mRNAs has different effects on menthol-evoked Ca^{2+} release. (**A** and **D**) Real-time quantification of TRPM8 F8/R9 and F21/R22 amplicon normalized to hypoxanthine-guanine phosphoribosyl transferase expression in PC-3 cells (**A**) or HEK-TRPM8 cells (**D**) transfected with 100 nM of control siRNA, siTRPM8-1, or siTRPM8-2. Each experiment was performed 6 times. (**B**, **C**, and **F**) Typical traces of the estimated ER Ca^{2+} release induced by 250 μM menthol in digitotin-permeabilized PC-3 (**B**), PrPE-20d (**C**), and HEK-TRPM8 cells (**F**). Insets show cumulative data (mean ± SEM) for percentage of menthol-evoked Ca^{2+} release from internal Ca^{2+} stores. Each condition included at least 40 cells from 3 independent experiments. (**E**) Cumulative data (mean ± SEM) of cold- and menthol-activated i_{TRPM8} in HEK-TRPM8 cells with control siRNA, siTRPM8-1, or siTRPM8-2 (currents recorded from voltage ramps at 100 mV). $^*P < 0.05$; $^{**}P < 0.01$; $^{***}P < 0.001$.

HEK-TRPM8 cells showed that siTRPM8-1 and siTRPM8-2 inhibited both $_{PM}$TRPM8 and $_{ER}$TRPM8 activity with the same efficiency (Figure 7, E and F, and Supplemental Figure 2, B and C).

Taken together, these results suggest that the truncated splice variant coding for the shorter, but still functional, TRPM8 isoform is expressed in AR-independent prostate epithelial cells. This truncated TRPM8 isoform is likely to represent ER-localized protein, which, in addition to functioning as an ER release channel, may also be responsible for the retention of the classic TRPM8 form in the ER, as was proposed for LNCaP cells (18).

Discussion

In this study, we report 4 major findings. First, primary epithelial cells from human NP, BPH, and PCa specimens exhibited classical cold/menthol receptor–like responses (i.e., characteristic of neuronal TRPM8) that were mediated by endogenous $_{PM}$TRPM8 activation. Second, the density of $_{PM}$TRPM8 membrane current increased in PCa in situ. Third, TRPM8 in PrPE cells also functioned as a Ca^{2+} release channel, $_{ER}$TRPM8. Finally, expression and activity of $_{ER}$TRPM8 and $_{PM}$TRPM8 depend on the differentiation and oncogenic status of prostate epithelial cells and are likely mediated by 2 TRPM8 isoforms that are differentially regulated by androgens.

Cold/menthol responsiveness of the human TRPM8 channel in prostate cells. This study is the first demonstration to our knowledge of functional $_{PM}$TRPM8 activity in human prostate cells. The biophysical properties of membrane current (strong outward rectification and close to 0 mV reversal potential) matched those of neuronal TRPM8 cold/menthol receptor–mediated current in PrPE and PrPCa cells (17, 27). Our siRNA-mediated TRPM8 knockout experiments proved the association of these responses with the expression of classical TRPM8 activity. In Ca^{2+} imaging experiments, menthol and icilin also induced $[Ca^{2+}]_c$ increases in PrPE cells. As was previously reported for LNCaP cells (18, 19), it should be noted that the menthol-evoked $[Ca^{2+}]_c$ increase in PrPE cells may be indicative of Ca^{2+} entry and SOCE via $_{PM}$TRPM8 and $_{ER}$TRPM8 activity, respectively. The distinct functions of $_{PM}$TRPM8 and $_{ER}$TRPM8 may be of great importance in understanding the physiology of prostate cells as well as other cells with dual TRPM8 localization.

Differential expression of $_{PM}$TRPM8 and $_{ER}$TRPM8 based on epithelial cell differentiation status and possible physiological roles of TRPM8 in NP cells. Prostate epithelium contains 3 types of epithelial cells: basal, TA/I, and apical/luminal (28, 29). The basal cells express CK14 and CK5 but not TRPM8 (16, 30); TA/I cells show a concomitant expression of basal marker CK5 and apical markers CK8/CK18 as well as low levels of AR and TRPM8 (16, 30). Apical cells (terminally differen-

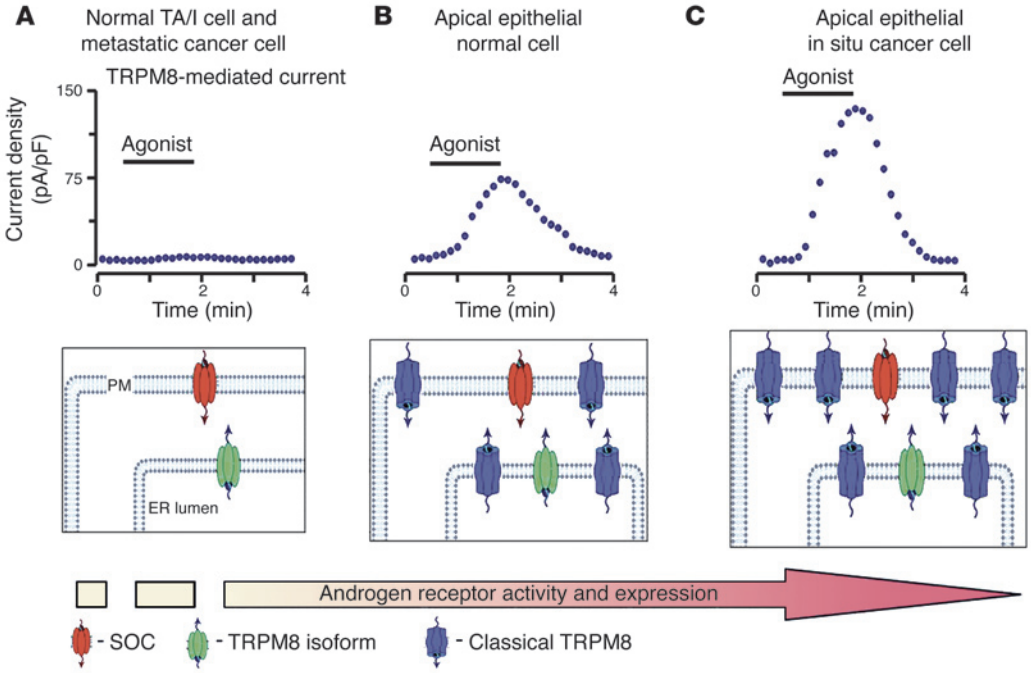

Figure 8

Schematic diagram summarizing the principal findings of this study and showing a simplified representation of differential TRPM8 localization and function depending on the AR activity, differentiation, and oncogenic status of human prostate epithelial cells. (**A**) General pattern of nondifferentiated TA/I cells and dedifferentiated metastatic cells. In these cells AR level was low, and only the $_{ER}$TRPM8 isoform was expressed in the ER membrane. $_{ER}$TRPM8 functioned as a Ca^{2+}-release ER channel, which, by depleting ER stores, activated SOC localized on the PM. Under these conditions, TRPM8 agonists did not induce classical $_{PM}$TRPM8-mediated current. (**B**) Normal, fully differentiated prostate cell with an apical secretory phenotype. In these cells, with high AR levels, the AR-dependent classical TRPM8 channel was expressed on both ER and PM. Under these conditions, TRPM8 agonists may induce not only SOCE, but also substantial $_{PM}$TRPM8-mediated current. (**C**) Differentiated apical secretory in situ cancer cells. In these cells, with enhanced AR activity, the AR-dependent classical TRPM8 channel was overexpressed and TRPM8 agonists induced high levels of $_{PM}$TRPM8-mediated current. i_{TRPM8} traces are schematic.

tiated secretory mature cells) express CK8/CK18 and PSA as well as high levels of AR and TRPM8 (16, 30). Moreover, our results showed that TRPM8 colocalized with CK18 (Figure 1C). It has previously been shown in kidney cells that TRP family member TRPP1 interacted directly with intermediated filament proteins, including CK18, which suggests that TRPP1 helps to stabilize epithelial cell sheets mechanically (31). It is also plausible that TRPM8 functions as an "epithelial phenotype stabilizer" in prostate epithelium.

Our results showed that PrPE-6d cells, which express the apical epithelial phenotype markers (16), exhibited both $_{PM}$TRPM8 and $_{ER}$TRPM8 activity, while the dedifferentiated PrPE-20d cells, which are characterized by the TA/I phenotype (23, 24), only conserved $_{ER}$TRPM8. Interestingly, only $_{ER}$TRPM8 activity has been observed in PC-3 cells, previously described to have common features with early TA/I cells (absence of AR, CK5, and CK18 expression) (32). Forced AR expression in PC-3 cells induced $_{PM}$TRPM8 function with the same kinetics as the expression of the PSA apical phenotype marker, suggesting that $_{PM}$TRPM8 is tightly regulated by the AR and appears during apical epithelial differentiation. Therefore, the loss of $_{PM}$TRPM8 function in TA/I cells was likely due to the loss of functional AR induced by dedifferentiation. AR regulation of $_{ER}$TRPM8 seems more complex. In PC-3 cells 3 days after AR transfection, Ca^{2+} release via $_{ER}$TRPM8 was apparently greater than that in control PC-3 cells, although the classical TRPM8 isoform was virtually undetectable and $_{PM}$TRPM8 was not functional. Furthermore, expression of the $_{ER}$TRPM8 isoform, mediating $_{ER}$TRPM8 activity, was considerably less sensitive to AR than was classical TRPM8 (Figure 5A). It will be necessary to clone this ER-specific TRPM8 isoform to understand its preferential targeting of the ER membrane and regulation by AR. The subject of the mechanism underlying androgen regulation of TRPM8 in the prostate has previously been addressed (13, 15, 16, 19), and several putative androgen response elements have been detected. However, an alternative promoter of *trpm8* may make the $_{ER}$TRPM8 isoform less sensitive to androgens than $_{PM}$TRPM8.

The observation that the $_{ER}$TRPM8 isoform is retained in the prostate cell ER membrane is also important for future research. Two scenarios have emerged on the basis of studies reporting ER retention of TRP channels: variations in TRP primary sequence (33) or partnership-evoked retention. For instance, subcellular localization and function of TRPP2, shown to act as a Ca^{2+} release ER channel, are controlled by phosphofurin acidic cluster sorting protein–1 (PACS-1) and PACS-2 (34). A reciprocal regulation between $_{ER}$TRPM8 and $_{PM}$TRPM8 is relatively likely and could also explain the retention of classical TRPM8 on the ER in LNCaP cells (18).

The physiological role of TRPM8 in the NP remains unknown. TA/I cells have been reported to be the most proliferative phenotype in NP epithelium (22), whereas apical cells are basically involved in the secretory activity of prostate acini. $_{ER}$TRPM8 activity may be involved in apical differentiation, while our data demonstrating specific $_{PM}$TRPM8 activity in human apical prostate cells suggest that the clas-

sical TRPM8 channel plays a role in the secretory function of prostate cells and is thereby indirectly involved in sperm motility and fertilization. Moreover, a cold receptor function of TRPM8 in the prostate was suggested by Stein et al. (35). This last hypothesis remains to be demonstrated since prostate is not physiologically exposed to low temperature. Finally, the results of recent studies demonstrating that phosphatidylinositol 4,5-bisphosphate tightly controls TRPM8 activity (36) emphasize the possibility that a membrane metabotropic receptor pathway may be involved in TRPM8 opening.

TRPM8 involvement in PCa. Early observations that TRPM8 upregulation correlated with the PCa stage led to the hypothesis that the *trpm8* gene was an oncogene (13–15), so TRPM8 was suggested as a putative target for anticancer therapies. Because AR has been reported to play an essential role in prostate carcinogenesis and TRPM8 is tightly regulated by AR, AR deregulation during PCa progression was expected to influence the physiological function of TRPM8. A convincing model of AR pathway evolution has recently been proposed (3), in which (a) AR regulates genes involved in the differentiation of secretory epithelial cells in normal prostate; (b) enhanced AR activity in the early stages of well-differentiated PCa activates growth-promoting genes and maintains apical epithelial phenotype; and (c) progression from high-grade PCa to metastasis is mediated by selective downregulation of the AR pathway genes. This downregulation results in a higher proliferation rate and enhances the potential to metastasize. Interestingly, in this study shows that the upregulation of the CK8 apical phenotype marker in PCa and its downregulation in metastasis coincide with our results on $_{PM}$TRPM8. Indeed, because intracapsular PCas are mainly composed of secretory apical cells (2) and metastatic cells are known to be close to the TA/I phenotype, we suggest that ARs play a key role in the development of $_{ER}$TRPM8 and $_{PM}$TRPM8 expression and activity during carcinogenesis of prostate cells (Figure 8).

Our data suggest that $_{PM}$TRPM8 and $_{ER}$TRPM8 may determine specific, oncogenic status–dependent Ca^{2+} signatures required for the progression of Ca^{2+}-dependent processes that are critical for carcinogenesis, such as proliferation (5, 37) and apoptosis (6, 9). Proliferation mostly relies on cytosolic Ca^{2+} signaling involving short, repeated Ca^{2+} entry mechanisms (37, 38). We therefore hypothesize that $_{PM}$TRPM8 is important for the Ca^{2+} signaling involved in proliferation. Moreover, store depletion and SOCE were previously shown to be critical in promoting growth arrest and apoptosis of PCa epithelial cells (7, 39). Indeed, reduced basal filling of intracellular Ca^{2+} stores is also the hallmark of the apoptosis-resistant cell phenotypes characteristic of advanced PCa (6, 9, 39). Thus, as $_{ER}$TRPM8 is a molecular entity capable of influencing the filling of ER stores, its activity may be considered a substantial factor in controlling the growth of advanced PCa metastatic cells. In light of the recent demonstration of the role of TRPM8 in LNCaP cell survival (19), we speculate that any shift in the balance between classical TRPM8 and $_{ER}$TRPM8 isoform expression may modify the Ca^{2+} signature, thus increasing the potential for either proliferation or apoptosis. Thus, TRPM8 may be an attractive target for therapeutic interventions: specific inhibition of either $_{ER}$TRPM8 or $_{PM}$TRPM8 activity should be considered, depending on the stage and androgen sensitivity of the targeted PCa. We believe these results provide novel insight and expect them to influence future research into the selective targeting of TRPM8 during PCa progression.

Methods

Cell cultures. HEK293 cells were cultured as described previously (18). PC-3 (Prostate Carcinoma; ATCC) were grown in RPMI 1684 (Invitrogen) supplemented with 10% fetal calf serum, L-glutamine (5 mM), and kanamycin (100 μg/ml).

Human prostate tissue specimens were obtained from resection surgeries performed on patients who gave informed consent and on clinical indications in the Urology Department at l'Hôpital St. Philibert. All specimens came from patients who had not received antiandrogen therapy. In addition, all specimens were diagnosed by an anatomopathological examination. After patient surgery, primary cells were prepared as described by Bidaux et al. (16).

All experiments on human tissues were approved by the Comité Consultatif de Protection des Personnes dans la Recherche Biomedicale de Lille (CCPPRB), Lille, France.

Transfection of siRNA. PrPE cells were transfected with 50 nM siTRPM8 (synthesized by Dharmacon) using 6 μl TransIT-TKO transfection reagent (Mirus Bio Corp.) according to the manufacturer's instructions. Sense sequences of siTRPM8-1 and siTRPM8-2 were 5′-UCUCUGAGCGCACUAUUCA(dTdT)-3′ and 5′-UAUCCGUCGGUCAUCUA(dTdT)-3′, respectively. These sequences are located at positions 894 and 2,736 on the TRPM8 mRNA (GenBank accession no. AY328400).

Heterologous overexpression. PC-3 cells were transfected with AR encoding vector using Nucleofector as recommended by the manufacturer (Amaxa).

Quantitative real-time PCR analysis. Expression levels of PCR products were quantified by quantitative real-time PCR on an ABI Prism 5700 Sequence Detection System. For each reaction, 10 ng of cDNA was placed in a 20-μl reaction mixture containing 12.5 μl of 2× QuantiTect SYBR Green PCR Master Mix (Applied Biosystems) and 300 nM of primer pairs (see Supplemental Table 1). TRPM8 mRNA levels were quantified with 2 different primer pairs, TRPM8(F8/R9) and TRPM8(F21/R22), whose sequences are presented in Supplemental Table 1. The housekeeping gene hypoxanthine-guanine phosphoribosyl transferase (HPRT) was used as an endogenous control to normalize variations in RNA extractions, the degree of RNA degradation, and variability in RT efficiency. To quantify the results we used the comparative threshold cycle method described by Livak and Schmittgen (40).

For single-cell real-time PCR, each cell fraction was split into 2 samples, which were submitted to reverse transcription with or without Moloney murine leukemia virus (MuLV) reverse transcriptase (Applied Biosystems). For analysis of real-time PCR, background contamination (samples without MuLV reverse transcription) was subtracted from the mRNA level of samples with MuLV transcription prior to calculation of the F8/R9-to-F21/R22 ratio.

Western blot assay. Total proteins from PC-3 cells were harvested in PBS, and then sonicated in an ice-cold buffer (pH 7.2) containing 10 mM PO_4Na_2/K buffer, 150 mM NaCl, 1 g/100 ml sodium deoxycholate, 1% Triton X-100, 1% NP40, a mixture of protease inhibitors (Sigma-Aldrich), and a phosphatase inhibitor (sodium orthovanadate; Sigma-Aldrich).

Prostate tissue membrane fractions were obtained by disrupting prostate resection specimens with a tissue homogenizer in an ice-cold lysis buffer containing 20 mM HEPES (pH 7.2), 25 mM sucrose, 0.1 mM EGTA, 5 mM EDTA, a mixture of protease inhibitors (Sigma-Aldrich), and a phosphatase inhibitor (sodium orthovanadate; Sigma-Aldrich). After 30 minutes of centrifugation at 30,000 *g* to remove the soluble protein fraction, the pellet was resuspended in the first buffer. After electrophoresis, proteins were transferred to a PVDF membrane using a semi-dry electroblotter (Bio-Rad). Immunoblotting was performed with primary rabbit polyclonal anti-TRPM8 antibody (diluted 1:2,000, catalog no. ab3243; Abcam) as described previously (16). The membrane was processed for chemiluminescence detection using Supersignal West Dura chemiluminescent substrate (Pierce) according to the manufacturer's instructions. Membranes were reblotted twice: first with mouse monoclonal anti-AR antibody (diluted 1:50, catalog no. ab9474; Abcam), and then with mouse monoclonal anti–pan-actin (diluted 1:500, catalog no. MS-1295-P; Neomarkers).

Electrophysiology and solutions. Membrane currents were recorded in the whole-cell configuration using the patch-clamp technique, together with

a computer-controlled EPC-9 amplifier (HEKA Electronic), as previously described (7). Patch pipettes were made on a P-97 puller (Sutter Instruments) from borosilicate glass capillaries (World Precision Instruments). For composition of extra- and intracellular solutions used, see Supplemental Table 2.

$[Ca^{2+}]_c$ measurements. $[Ca^{2+}]_c$ was measured using Fluo-4 AM dye, as previously described (18), in the same normal extracellular solution used for electrophysiological recordings of i_{TRPM8}. To produce Ca^{2+}-free conditions, $CaCl_2$ was removed from this solution and 0.5 mM EGTA was added.

$[Ca^{2+}]_{ER}$ measurements. $[Ca^{2+}]_{ER}$ was measured using Mag–Fluo-4 AM dye, as previously described (18). Ratio imaging of Mag–Fluo-4 was measured using a confocal microscope (LSM 510; Zeiss).

Statistics. Electrophysiological data were analyzed using PulseFit (version 8.31; HEKA Electronics), pCLAMP (version 8; Axon Instruments), and Origin (version 7.0; Microcal) software. Results were expressed as mean ± SEM unless otherwise indicated. Student's *t* test was used for statistical comparison of the differences, and $P < 0.05$ was considered significant.

See supplemental methods for the creation of HEK-293 cell line, recombinant protein preparation, RT-PCR, and immunohistochemistry.

Acknowledgments

This work was supported by grants from INSERM; Ministère de l'Education Nationale; and La Ligue Nationale Contre le Cancer, la region Nord/Pas-de-Calais. Y. Shuba was supported by a grant from INTAS (011-8223). D. Gkikia was supported by a long-term fellowship from the European Molecular Biology Organization (ALTF-161-2006).

Received for publication August 25, 2006, and accepted in revised form March 20, 2007.

Address correspondence to: Natalia Prevarskaya, Laboratoire de Physiologie Cellulaire, INSERM U800, Bâtiment SN3, USTL, Villeneuve d'Ascq 59655, France. Phone: 33-3-20-43-40-77; Fax: 33-3-20-43-40-66; E-mail: natacha.prevarskaya@univ-lille1.fr.

Gabriel Bidaux and Matthieu Flourakis contributed equally to this work.

1. Reya, T., Morrison, S.J., Clarke, M.F., and Weissman, I.L. 2001. Stem cells, cancer, and cancer stem cells. *Nature.* **414**:105–111.
2. Schalken, J.A., and van Leenders, G. 2003. Cellular and molecular biology of the prostate: stem cell biology. *Urology.* **62**:11–20.
3. Hendriksen, P.J., et al. 2006. Evolution of the androgen receptor pathway during progression of prostate cancer. *Cancer Res.* **66**:5012–5020.
4. Legrand, G., et al. 2001. Ca2+ pools and cell growth. Evidence for sarcoendoplasmic Ca2+-ATPases 2B involvement in human prostate cancer cell growth control. *J. Biol. Chem.* **276**:47608–47614.
5. Thebault, S., et al. 2006. Differential role of transient receptor potential channels in Ca2+ entry and proliferation of prostate cancer epithelial cells. *Cancer Res.* **66**:2038–2047.
6. Vanoverberghe, K., et al. 2004. Ca2+ homeostasis and apoptotic resistance of neuroendocrine-differentiated prostate cancer cells. *Cell Death Differ.* **11**:321–330.
7. Skryma, R., et al. 2000. Store depletion and store-operated Ca2+ current in human prostate cancer LNCaP cells: involvement in apoptosis. *J. Physiol.* **527**:71–83.
8. Vanden Abeele, F., Roudbaraki, M., Shuba, Y., Skryma, R., and Prevarskaya, N. 2003. Store-operated Ca2+ current in prostate cancer epithelial cells. Role of endogenous Ca2+ transporter type 1. *J. Biol. Chem.* **278**:15381–15389.
9. Vanden Abeele, F., et al. 2002. Bcl-2-dependent modulation of Ca(2+) homeostasis and store-operated channels in prostate cancer cells. *Cancer Cell.* **1**:169–179.
10. Montell, C., Birnbaumer, L., and Flockerzi, V. 2002. The TRP channels, a remarkably functional family. *Cell.* **108**:595–598.
11. Zhang, L., and Barritt, G.J. 2006. TRPM8 in prostate cancer cells: a potential diagnostic and prognostic marker with a secretory function? *Endocr. Relat. Cancer.* **13**:27–38.
12. Kiessling, A., et al. 2003. Identification of an HLA-A*0201-restricted T-cell epitope derived from the prostate cancer-associated protein trp-p8. *Prostate.* **56**:270–279.
13. Tsavaler, L., Shapero, M.H., Morkowski, S., and Laus, R. 2001. Trp-p8, a novel prostate-specific gene, is up-regulated in prostate cancer and other malignancies and shares high homology with transient receptor potential calcium channel proteins. *Cancer Res.* **61**:3760–3769.
14. Fuessel, S., et al. 2003. Multiple tumor marker analyses (PSA, hK2, PSCA, trp-p8) in primary prostate cancers using quantitative RT-PCR. *Int. J. Oncol.* **23**:221–228.
15. Henshall, S.M., et al. 2003. Survival analysis of genome-wide gene expression profiles of prostate cancers identifies new prognostic targets of disease relapse. *Cancer Res.* **63**:4196–4203.
16. Bidaux, G., et al. 2005. Evidence for specific TRPM8 expression in human prostate secretory epithelial cells: functional androgen receptor requirement. *Endocr. Relat. Cancer.* **12**:367–382.
17. McKemy, D.D., Neuhausser, W.M., and Julius, D. 2002. Identification of a cold receptor reveals a general role for TRP channels in thermosensation. *Nature.* **416**:52–58.
18. Thebault, S., et al. 2005. Novel role of cold/menthol-sensitive transient receptor potential melastatine family member 8 (TRPM8) in the activation of store-operated channels in LNCaP human prostate cancer epithelial cells. *J. Biol. Chem.* **280**:39423–39435.
19. Zhang, L., and Barritt, G.J. 2004. Evidence that TRPM8 is an androgen-dependent Ca2+ channel required for the survival of prostate cancer cells. *Cancer Res.* **64**:8365–8373.
20. Erler, I., et al. 2006. Trafficking and assembly of the cold-sensitive TRPM8 channel. *J. Biol. Chem.* **281**:38396–38404.
21. Wang, S., et al. 2006. Pten deletion leads to the expansion of a prostatic stem/progenitor cell subpopulation and tumor initiation. *Proc. Natl. Acad. Sci. U. S. A.* **103**:1480–1485.
22. Garraway, L.A., et al. 2003. Intermediate basal cells of the prostate: in vitro and in vivo characterization. *Prostate.* **55**:206–218.
23. Planz, B., et al. 2004. Studies on the differentiation pathway and growth characteristics of epithelial culture cells of the human prostate. *Prostate Cancer Prostatic Dis.* **7**:73–83.
24. Uzgare, A.R., Xu, Y., and Isaacs, J.T. 2004. In vitro culturing and characteristics of transit amplifying epithelial cells from human prostate tissue. *J. Cell. Biochem.* **91**:196–205.
25. Whitacre, D.C., et al. 2002. Androgen induction of in vitro prostate cell differentiation. *Cell Growth Differ.* **13**:1–11.
26. Zegarra-Moro, O.L., Schmidt, L.J., Huang, H., and Tindall, D.J. 2002. Disruption of androgen receptor function inhibits proliferation of androgen-refractory prostate cancer cells. *Cancer Res.* **62**:1008–1013.
27. Peier, A.M., et al. 2002. A TRP channel that senses cold stimuli and menthol. *Cell.* **108**:705–715.
28. van Leenders, G.J., et al. 2003. Intermediate cells in human prostate epithelium are enriched in proliferative inflammatory atrophy. *Am. J. Pathol.* **162**:1529–1537.
29. Bonkhoff, H., and Remberger, K. 1996. Differentiation pathways and histogenetic aspects of normal and abnormal prostatic growth: a stem cell model. *Prostate.* **28**:98–106.
30. van Leenders, G.J., and Schalken, J.A. 2003. Epithelial cell differentiation in the human prostate epithelium: implications for the pathogenesis and therapy of prostate cancer. *Crit. Rev. Oncol. Hematol.* **46**(Suppl.):S3–S10.
31. Xu, G.M., et al. 2001. Polycystin-1 interacts with intermediate filaments. *J. Biol. Chem.* **276**:46544–46552.
32. van Leenders, G.J., Aalders, T.W., Hulsbergen-van de Kaa, C.A., Ruiter, D.J., and Schalken, J.A. 2001. Expression of basal cell keratins in human prostate cancer metastases and cell lines. *J. Pathol.* **195**:563–570.
33. Arniges, M., Fernandez-Fernandez, J.M., Albrecht, N., Schaefer, M., and Valverde, M.A. 2006. Human TRPV4 channel splice variants revealed a key role of ankyrin domains in multimerization and trafficking. *J. Biol. Chem.* **281**:1580–1586.
34. Kottgen, M., et al. 2005. Trafficking of TRPP2 by PACS proteins represents a novel mechanism of ion channel regulation. *EMBO J.* **24**:705–716.
35. Stein, R.J., et al. 2004. Cool (TRPM8) and hot (TRPV1) receptors in the bladder and male genital tract. *J. Urol.* **172**:1175–1178.
36. Rohacs, T., Lopes, C.M., Michailidis, I., and Logothetis, D.E. 2005. PI(4,5)P2 regulates the activation and desensitization of TRPM8 channels through the TRP domain. *Nat. Neurosci.* **8**:626–634.
37. Thebault, S., et al. 2003. α1-adrenergic receptors activate Ca^{2+}-permeable cationic channels in prostate cancer epithelial cells. *J. Clin. Invest.* **111**:1691–1701. doi:10.1172/JCI200316293.
38. Berridge, M.J. 2001. The versatility and complexity of calcium signalling. *Novartis Found. Symp.* **239**:52–64; discussion 64–57, 150–159.
39. Prevarskaya, N., Skryma, R., and Shuba, Y. 2004. Ca2+ homeostasis in apoptotic resistance of prostate cancer cells. *Biochem. Biophys. Res. Commun.* **322**:1326–1335.
40. Livak, K.J., and Schmittgen, T.D. 2001. Analysis of relative gene expression data using real-time quantitative PCR and the 2(-Delta Delta C(T)) method. *Methods.* **25**:402–408.